

## Supporting Information - Doping Effects on the Geometric and Electronic Structure of Tin Clusters

Martin Gleditzsch<sup>\*a</sup>, Marc Jäger<sup>a</sup>, Lukáš F. Paštka<sup>b</sup>, Armin Shayeghi<sup>c</sup> and Rolf Schäfer<sup>a</sup>

### 1 Electric Deflection Measurements

The target was prepared with a low atom percentage of copper in tin in order to reduce possible multi doping. Since mass signal overlapping with neighbouring species can result in a slight modification of the beam profile, the beam profiles have been carefully evaluated for different peak integration limits. Because the deflection behaviour was consistent for narrow and wide limits, the mass peaks are considered to contain no significant multi-doped fractions. Fig. 1 displays an exemplary mass spectrum for an alloy target with 5 atom-% Cu in Sn at 20 K nozzle temperature. The broad isotopic distribution of tin and multi-doped species result in a relatively high noise-to-signal-ratio, which is more pronounced for targets with higher copper contribution. While tracers of  $\text{Sn}_7\text{Cu}$  and  $\text{Sn}_8\text{Cu}$  are visible, it was not possible to stabilize their corresponding mass peaks during beam deflection measurements.  $\text{Sn}_9\text{Cu}$  is the first stable doped cluster during electric beam deflection measurement. Starting with  $\text{Sn}_{10}\text{Cu}$  the clusters are equally or more stable than the pure tin clusters. Interestingly, it was not possible to record any mass peaks for  $\text{Sn}_{17}\text{Cu}$ . Fig. 2 illustrates the influence of the rotational temperature  $T_{\text{rot}}$  exemplary on two electric beam deflection simulations. The influence of  $T_{\text{rot}}$  on the simulated beam profile is shown to be only minor in the range 5 – 25 K. Thus, the assumption  $T_{\text{rot}} = 10$  K is appropriate and employed for all simulations shown in the main text. Fig. 3 describes thermal excitation of the clusters within a simple two-component fit model, where the rigid fraction  $P_0$  is exhibiting the full ground state dipole moment and the second fraction  $P_1$  is assumed to be flexible, resulting in a vanishing dipole moment. The clusters  $\text{Sn}_{11}\text{Cu}$  ( $P_1 = 55\%$ ) and  $\text{Sn}_{13}\text{Cu}$  ( $P_1 = 53\%$ ) are slightly more excited than  $\text{Sn}_{16}\text{Cu}$  ( $P_1 = 43\%$ ). This agrees with the observation that species with higher absolute values for the electric dipole moment appear to be more sensitive to thermal excitation.

### 2 Quantum Chemistry

Fig. 4 shows all energetically low-lying isomers up to 0.5 eV for  $\text{Sn}_N\text{Cu}$  with  $N = 9\text{--}16$ . All structures have been obtained by optimizing the GA generated candidates on the PBE0/cc-pVTZ-PP level of theory. All energetic low lying structures were found to display doublet multiplicity, as their quartet counterparts were significantly higher in energy. The corresponding properties are summarized in table 1. The first column contains the label as shown in Figure 4.  $\Delta E$  refers to the energy relative to the identified global minimum structure in eV, which is followed by the column for the point group symmetry (Symm.). The isotropic polarizability is shown in  $\text{\AA}^3$  per number of atoms. The columns for the total magnitude of the electric dipole moment  $\mu_{\text{tot}}$  and its components  $\mu_i$  ( $i = x, y, z$ ) are displayed in Debye (D). They are given in the same molecular fixed frame like the moment of inertia components  $I_i$  ( $i = x, y, z$ ), which are expressed with respect to the smallest component  $I_{\text{min}}$  in  $\text{kg m}^2 \cdot 10^{-44}$ .

The partial charges calculated with a range of different techniques are shown for the dopant of the GS in table 2. While the absolute values of the partial charges are not consistent, they unambiguously predict a negative sign and thus an electron transfer from the tin cage to the copper dopant. The electron density is consistently low regarding all methods, which confirms the presence of an electron transfer. The DDEC6 results for  $\text{Sn}_{12}\text{Mn}$  yield a slightly positive partial charge  $\delta(\text{Mn}) = 0.08$  and a spin density of  $\rho(\text{Mn}) = 4.30$  at the dopant. The tables 3 till 5 show the frontier Molecular Orbital (MO) composition for  $\text{Sn}_{12}\text{M}$  with  $\text{M} = \text{Mn}, \text{Cu}, \text{Au}$  in the range of  $-(10.2\text{--}2.82)$  eV on the PBE0/cc-pVTZ-PP level of theory. While for the dopant only equivalent atomic orbitals (AO) have been summarized, for the tin cage atoms the table has been additionally simplified by AO summation over all tin atoms.

<sup>a</sup> Technische Universität Darmstadt, Eduard-Zintl-Institut, Alarich-Weiss-Straße 8, 64287 Darmstadt, Germany

<sup>b</sup> Department of Physical and Theoretical Chemistry & Laboratory for Advanced Materials, Faculty of Natural Sciences, Comenius University, Mlynská dolina, Ilkovičova 6, 84215 Bratislava, Slovakia

<sup>c</sup> Vienna Center for Quantum Science and Technology (VCQ), Faculty of Physics, University of Vienna, Boltzmanngasse 5, A-1090 Vienna, Austria

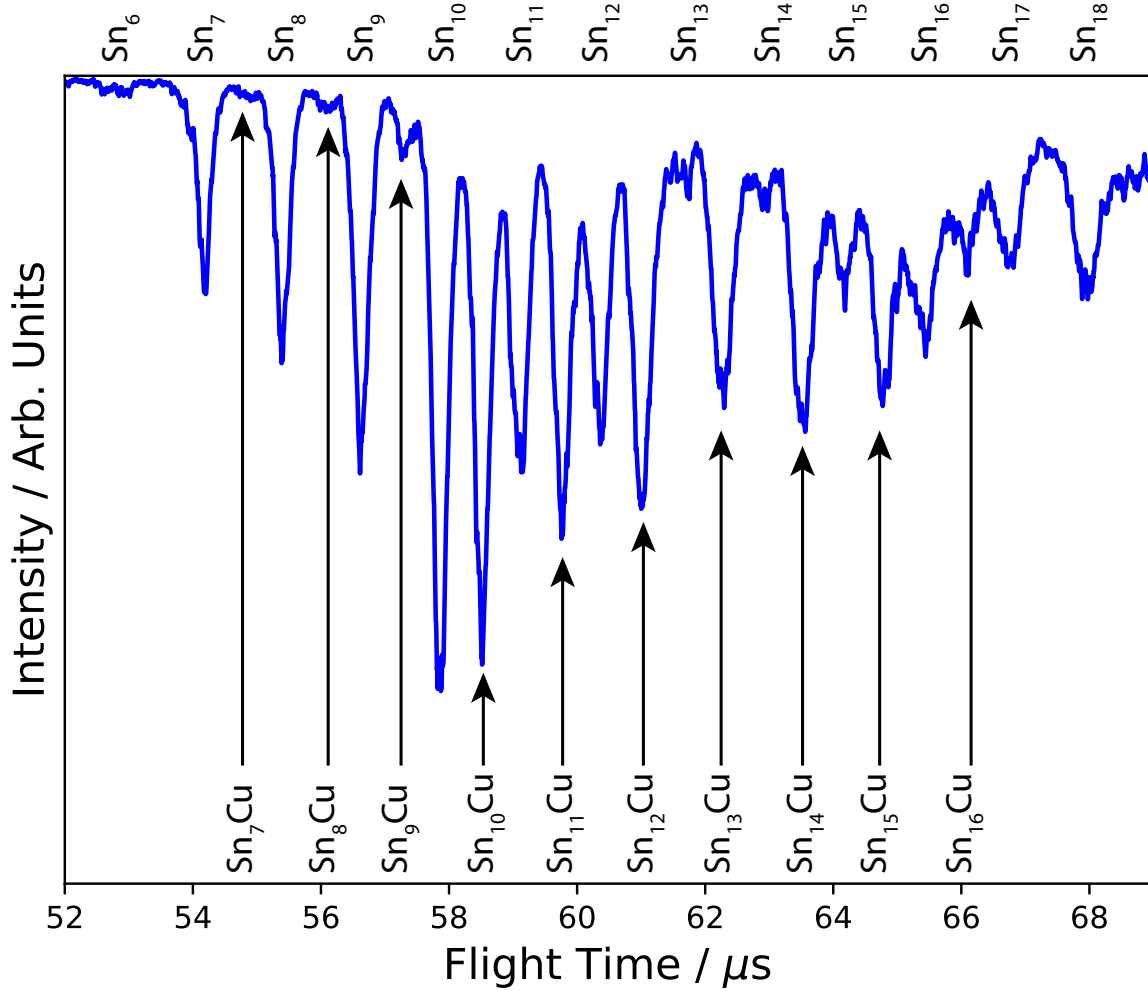


**Fig. 1** Mass spectrum of copper-doped tin clusters  $\text{Sn}_N\text{Cu}$  for an alloy target (5 atom-% Cu in Sn) at 20 K nozzle temperature. The mass signals for pure tin clusters are shown as reference. While tracers of  $\text{Sn}_7\text{Cu}$  and  $\text{Sn}_8\text{Cu}$  are visible, they are not stable during the beam deflection measurements. Interestingly,  $\text{Sn}_{17}\text{Cu}$  vanishes in the baseline and cannot be recorded.

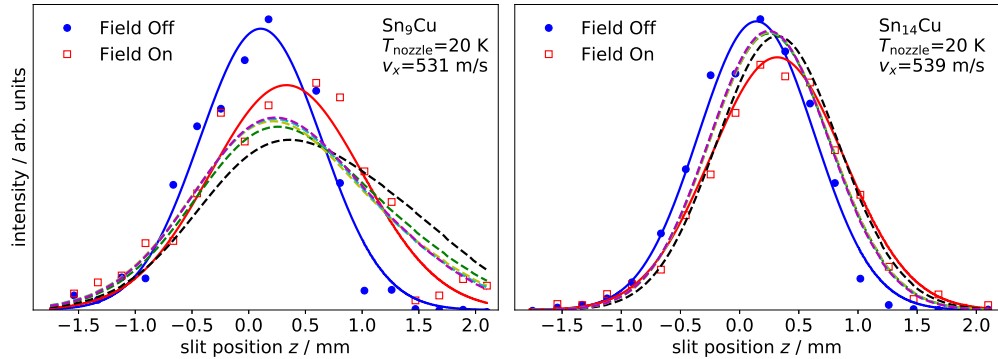


**Fig. 2** Comparison of experimental electric deflection results with field switched off (blue) and on (red) with the simulated beam profiles for different rotational temperatures ( $T_{\text{rot}}$ ). The influence on a rigid rotor is shown to be only minor in the range of 5-25 K. The colour notation is black (5 K), green (10 K), yellow (15 K), cyan (20 K) and magenta (25 K).

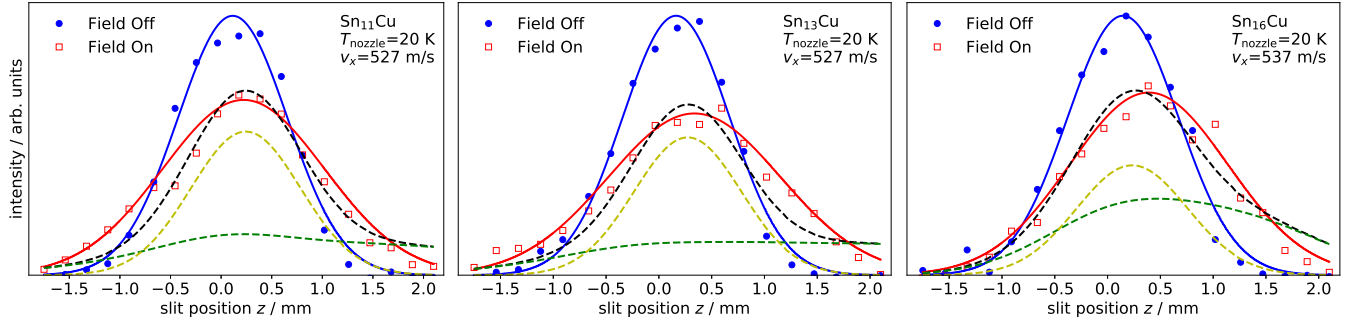


**Fig. 3** Simulated beam profiles of the simple two-component-fit model with the ground state  $P_0$  fraction displaying the full DFT dipole moment and with  $P_1$  referring to a flexible fraction of the cluster with a vanishing dipole moment. The colour notation is black for the combined beam profile, yellow for  $P_1$  multiplied with the fully excited beam profile and green for  $(1 - P_1)$  multiplied with the GS beam profile. The clusters  $\text{Sn}_{11}\text{Cu}$  ( $P_1 = 55\%$ ) and  $\text{Sn}_{13}\text{Cu}$  ( $P_1 = 53\%$ ) are slightly more excited than  $\text{Sn}_{16}\text{Cu}$  ( $P_1 = 43\%$ ). This agrees with the observation that species with higher absolute values for the electric dipole moment appear to be more sensitive to thermal excitation.

**Table 1** Results of the DFT studies for  $\text{Sn}_N\text{Cu}$  on the PBE0/cc-pVTZ-PP level of theory. The structures are visualized in Fig. 4 and exhibit doublet spin multiplicity.

Label	$\Delta E/\text{eV}$	Symm.	$\frac{\alpha}{\text{\AA}^3/\text{N}_{\text{atoms}}}$	$\mu_{\text{tot}}/\text{D}$	$\mu_x/\text{D}$	$\mu_y/\text{D}$	$\mu_z/\text{D}$	$I_{\text{min}}$ ( $\text{kg}\cdot\text{m}^2\cdot 10^{-44}$ )	$I_x/I_{\text{min}}$	$I_y/I_{\text{min}}$	$I_z/I_{\text{min}}$
9-I	0.00	$C_s$	6.66	0.35	0.00	0.28	-0.30	7.933	1.000	1.028	1.274
10-I	0.00	$D_{4d}$	6.42	0.00	0.00	0.00	0.00	9.324	1.000	1.101	1.101
11-I	0.00	$C_{2v}$	6.52	1.00	0.00	-1.00	0.00	10.692	1.000	1.173	1.215
11-II	0.19	$C_s$	6.67	1.31	-1.26	-0.33	0.00	9.889	1.000	1.347	1.445
11-III	0.26	$C_1$	6.68	1.22	-1.11	0.51	0.03	10.748	1.000	1.144	1.318
12-I	0.00	$D_{5d}$	6.38	0.00	0.00	0.00	0.00	13.595	1.000	1.000	1.042
13-I	0.00	$C_s$	6.59	1.22	-1.19	0.00	0.30	14.114	1.000	1.253	1.260
13-II	0.36	$C_1$	6.78	1.67	-1.65	0.24	-0.20	12.881	1.000	1.445	1.591
13-III	0.37	$C_s$	6.92	0.45	0.00	0.24	0.37	12.571	1.000	1.520	1.707
13-IV	0.42	$C_{2v}$	6.75	0.17	0.17	0.00	0.00	12.434	1.000	1.521	1.642
13-V	0.46	$C_s$	6.82	1.61	-1.51	0.00	0.56	14.883	1.000	1.089	1.388
14-I	0.00	$C_1$	6.80	0.19	-0.04	-0.02	0.18	14.337	1.000	1.530	1.635
14-II	0.16	$C_1$	6.64	0.42	-0.17	0.14	0.36	15.174	1.000	1.336	1.437
14-III	0.36	$C_s$	6.82	0.76	0.76	0.00	0.00	13.346	1.000	1.761	1.761
14-IV	0.39	$C_2$	6.86	0.56	0.00	-0.56	0.00	15.662	1.000	1.330	1.456
15-I	0.00	$C_s$	6.69	0.47	0.15	0.00	0.45	17.245	1.000	1.388	1.391
15-II	0.11	$C_1$	6.87	0.92	-0.91	-0.03	0.00	15.232	1.000	1.750	1.793
15-III	0.42	$C_s$	6.63	1.09	0.65	0.87	0.00	18.039	1.000	1.262	1.296
15-IV	0.44	$C_s$	6.83	0.29	-0.21	-0.01	-0.20	16.278	1.000	1.572	1.584
16-I	0.00	$C_s$	6.93	0.94	0.89	0.00	-0.31	17.524	1.000	1.730	1.731
16-II	0.37	$C_s$	6.80	1.00	-0.99	-0.01	-0.15	17.717	1.000	1.598	1.675
16-III	0.31	$C_s$	7.29	2.17	-2.16	-0.20	0.00	16.447	1.000	2.060	2.075
16-IV	0.35	$C_1$	6.84	0.29	-0.07	0.07	0.27	21.315	1.000	1.137	1.341
16-V	0.43	$C_1$	6.87	0.40	0.30	0.00	0.27	19.823	1.000	1.301	1.479
16-VI	0.44	$C_s$	6.69	0.55	-0.40	0.00	-0.37	20.589	1.000	1.202	1.335
16-VII	0.44	$C_1$	6.69	1.44	-0.65	1.22	0.42	21.641	1.000	1.078	1.244

**Table 2** Results of the ground state partial charge analysis for  $\text{Sn}_N\text{Cu}$  on the PBE0/cc-pVTZ-PP level of theory. Here  $\delta_i$  are the partial charges (or net atomic charges, NACs) in elementary charge and  $\rho_i$  the total spin density on the copper dopant for 'density derived Electrostatic and chemical approach' (DDEC6), Löwdin (Löw), Natural Charge (Nat) and Bader analysis, respectively.

$N$	$\delta_{\text{DDEC6}}$	$\rho_{\text{DDEC6}}$	$\delta_{\text{Löw}}$	$\rho_{\text{Löw}}$	$\delta_{\text{Nat}}$	$\rho_{\text{Nat}}$	$\delta_{\text{Bad.}}$
9	-0.16	0.10	-0.83	0.11	-1.96	0.14	-0.53
10	-0.20	0.02	-0.89	0.03	-2.28	0.06	-0.62
11	-0.17	-0.02	-0.85	-0.01	-1.94	0.01	-0.52
12	-0.17	-0.01	-0.77	0.00	-1.45	0.04	-0.32
13	-0.16	0.01	-0.76	0.00	-1.41	0.00	-0.32
14	-0.15	-0.01	-0.85	0.00	-1.93	0.00	-0.52
15	-0.14	0.00	-0.76	0.01	-1.30	0.01	-0.34
16	-0.11	0.00	-0.82	0.01	-1.88	0.03	-0.45

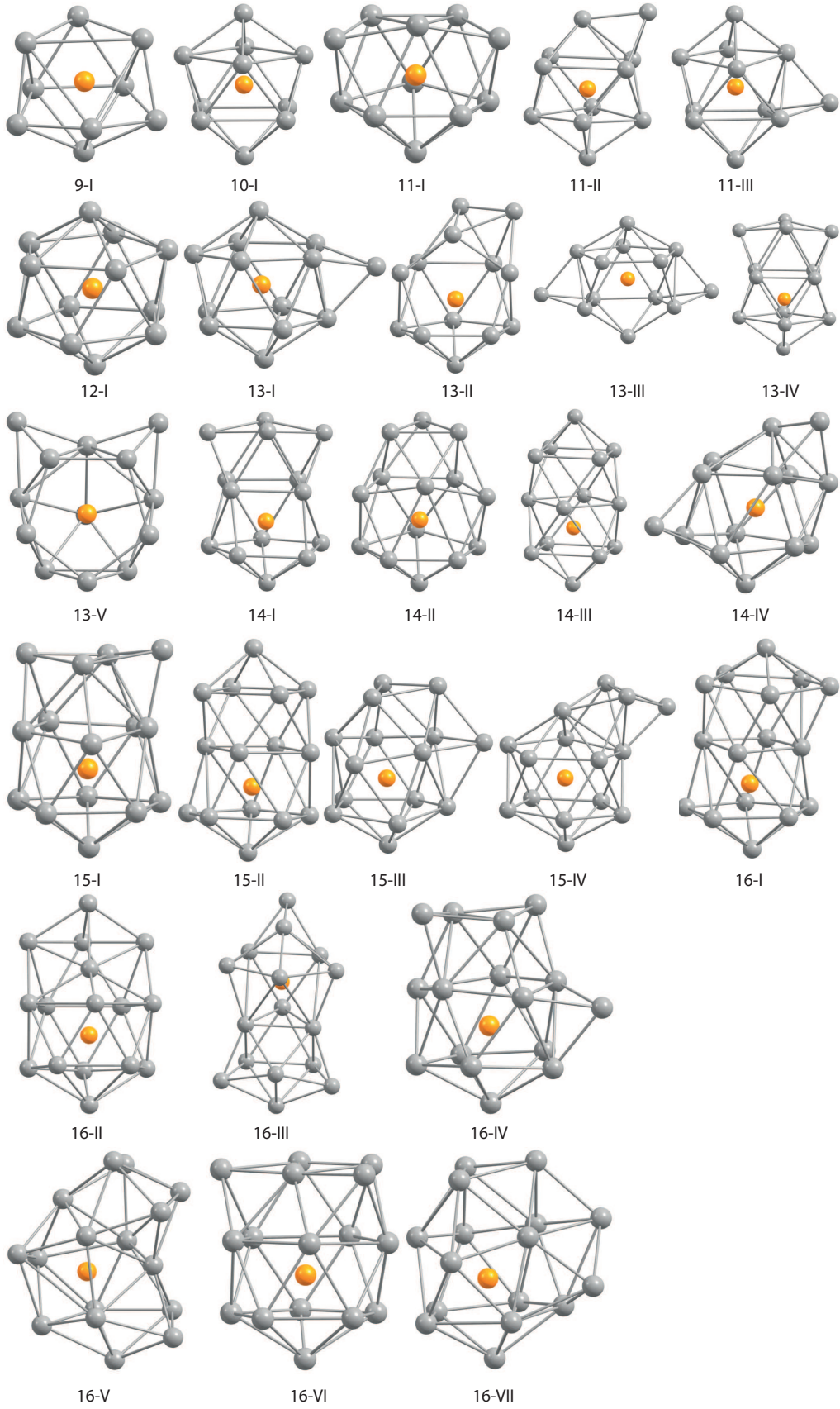


**Fig. 4** Energetically low-lying isomers up to 0.5 eV for the single-doped  $\text{Sn}_N\text{Cu}$  clusters with  $N = 9\text{-}16$  as obtained at the PBE0/cc-pVTZ-PP level of theory. Below each structure, the number of tin atoms and the order of the isomer (Roman numeral) is denoted. Their properties are summarized in table 1.

**Table 3** Molecular orbital composition for Sn<sub>12</sub>Mn in the range of -(10.2-2.82) eV on the PBE0/cc-pVTZ-PP level of theory. The absolute coefficients are displayed, equivalent atomic orbitals (AO) and ligands have been summarized.

Label	E/eV	Mn-3s	Mn-3p	Mn-3d	Mn-4s	Mn-4p	Mn-4d	Sn-4s	Sn-4p	Sn-4d	Sn-4f	Sn-5s	Sn-5p	Sn-5d
1T <sub>u</sub> α-Mn	-10.052	0.00	0.00	0.00	0.00	0.00	0.00	0.00	0.02	0.54	0.02	2.14	0.38	0.32
1T <sub>u</sub> α-Mn	-10.052	0.00	0.00	0.00	0.00	0.00	0.00	0.00	0.02	0.62	0.02	2.26	0.40	0.34
1T <sub>u</sub> α-Mn	-10.052	0.00	0.00	0.00	0.00	0.00	0.00	0.00	0.02	0.50	0.06	2.14	0.40	0.26
2H <sub>g</sub> α-Mn	-9.905	0.00	0.00	1.97	0.00	0.00	0.05	0.00	0.00	0.18	0.00	0.74	1.04	0.10
2H <sub>g</sub> α-Mn	-9.905	0.00	0.00	2.02	0.00	0.00	0.04	0.00	0.00	0.28	0.02	0.86	1.04	0.12
2H <sub>g</sub> α-Mn	-9.905	0.00	0.00	2.08	0.00	0.00	0.04	0.00	0.00	0.22	0.02	0.76	0.98	0.10
2H <sub>g</sub> α-Mn	-9.905	0.00	0.00	2.02	0.00	0.00	0.04	0.00	0.00	0.22	0.02	0.80	1.08	0.10
2H <sub>g</sub> α-Mn	-9.905	0.00	0.00	2.13	0.00	0.00	0.05	0.00	0.00	0.20	0.02	0.66	1.00	0.10
3A <sub>g</sub> α-Mn	-8.441	0.12	0.00	0.03	0.22	0.00	0.12	0.00	0.08	0.94	0.40	0.96	3.42	0.18
4G <sub>u</sub> α-Mn	-7.105	0.00	0.00	0.00	0.00	0.00	0.00	0.00	0.00	0.74	0.22	0.00	4.78	0.06
4G <sub>u</sub> α-Mn	-7.105	0.00	0.00	0.00	0.00	0.00	0.00	0.00	0.00	0.76	0.34	0.00	5.14	0.00
4G <sub>u</sub> α-Mn	-7.105	0.00	0.00	0.00	0.00	0.00	0.00	0.00	0.00	0.74	0.28	0.00	4.94	0.06
4G <sub>u</sub> α-Mn	-7.105	0.00	0.00	0.00	0.00	0.00	0.00	0.00	0.00	0.72	0.28	0.00	5.06	0.12
5T <sub>u</sub> α-Mn	-6.305	0.00	0.85	0.00	0.00	0.48	0.00	0.00	0.00	0.76	0.28	0.68	3.66	0.10
5T <sub>u</sub> α-Mn	-6.305	0.00	0.76	0.00	0.00	0.43	0.00	0.00	0.00	0.68	0.34	0.68	4.42	0.16
5T <sub>u</sub> α-Mn	-6.305	0.00	0.93	0.00	0.00	0.54	0.00	0.00	0.00	0.66	0.34	0.66	4.16	0.18
6H <sub>g</sub> α-Mn	-5.548	0.00	0.00	0.35	0.00	0.00	0.00	0.02	0.00	0.52	0.42	0.74	6.02	0.08
6H <sub>g</sub> α-Mn	-5.548	0.00	0.00	0.34	0.00	0.00	0.00	0.00	0.00	0.42	0.42	1.02	5.80	0.10
6H <sub>g</sub> α-Mn	-5.548	0.00	0.00	0.37	0.00	0.00	0.00	0.00	0.00	0.50	0.36	0.84	5.64	0.08
6H <sub>g</sub> α-Mn	-5.548	0.00	0.00	0.37	0.00	0.00	0.00	0.00	0.00	0.44	0.32	1.04	4.92	0.12
6H <sub>g</sub> α-Mn	-5.548	0.00	0.00	0.37	0.00	0.00	0.02	0.00	0.48	0.30	0.72	5.22	0.10	
1T <sub>u</sub> β-Mn	-10.008	0.00	0.00	0.00	0.00	0.00	0.00	0.02	0.52	0.02	2.12	0.44	0.32	
1T <sub>u</sub> β-Mn	-10.008	0.00	0.00	0.00	0.00	0.00	0.00	0.02	0.62	0.02	2.24	0.44	0.34	
1T <sub>u</sub> β-Mn	-10.006	0.00	0.00	0.00	0.00	0.00	0.00	0.02	0.48	0.06	2.12	0.42	0.24	
2A <sub>g</sub> β-Mn	-8.114	0.09	0.00	0.00	0.17	0.00	0.03	0.00	0.10	0.82	0.46	0.96	3.72	0.14
3G <sub>u</sub> β-Mn	-6.928	0.00	0.00	0.00	0.00	0.00	0.00	0.00	0.00	0.72	0.26	0.00	4.70	0.06
3G <sub>u</sub> β-Mn	-6.928	0.00	0.00	0.00	0.00	0.00	0.00	0.00	0.00	0.76	0.30	0.00	5.06	0.06
3G <sub>u</sub> β-Mn	-6.928	0.00	0.00	0.00	0.00	0.00	0.00	0.00	0.00	0.76	0.28	0.00	5.12	0.08
3G <sub>u</sub> β-Mn	-6.928	0.00	0.00	0.00	0.00	0.00	0.00	0.00	0.00	0.72	0.38	0.00	5.08	0.16
4T <sub>u</sub> β-Mn	-6.289	0.00	1.03	0.00	0.00	0.75	0.00	0.00	0.00	0.72	0.30	0.68	3.68	0.14
4T <sub>u</sub> β-Mn	-6.289	0.00	0.94	0.00	0.00	0.68	0.00	0.00	0.00	0.62	0.38	0.70	4.58	0.16
4T <sub>u</sub> β-Mn	-6.289	0.00	1.14	0.00	0.00	0.83	0.00	0.00	0.00	0.66	0.42	0.66	4.26	0.16
5H <sub>g</sub> β-Mn	-5.856	0.00	0.00	0.50	0.00	0.00	0.06	0.00	0.00	0.58	0.38	0.74	5.44	0.10
5H <sub>g</sub> β-Mn	-5.856	0.00	0.00	0.48	0.00	0.00	0.05	0.00	0.00	0.58	0.48	0.98	5.32	0.16
5H <sub>g</sub> β-Mn	-5.853	0.00	0.00	0.53	0.00	0.00	0.05	0.02	0.00	0.52	0.38	0.80	5.16	0.12
5H <sub>g</sub> β-Mn	-5.853	0.00	0.00	0.50	0.00	0.00	0.06	0.00	0.00	0.50	0.40	1.04	5.10	0.16
5H <sub>g</sub> β-Mn	-5.853	0.00	0.00	0.47	0.00	0.00	0.06	0.00	0.00	0.52	0.38	0.76	4.82	0.10
6H <sub>g</sub> β-Mn	-2.819	0.00	0.00	1.00	0.00	0.00	0.11	0.00	0.08	0.70	0.36	0.46	4.12	0.16
6H <sub>g</sub> β-Mn	-2.819	0.00	0.00	1.23	0.00	0.00	0.14	0.00	0.06	0.66	0.42	0.62	4.16	0.16
6H <sub>g</sub> β-Mn	-2.819	0.00	0.00	1.07	0.00	0.00	0.12	0.00	0.08	0.74	0.38	0.48	4.08	0.16
6H <sub>g</sub> β-Mn	-2.819	0.00	0.00	1.28	0.00	0.00	0.15	0.00	0.04	0.66	0.40	0.50	4.12	0.22
6H <sub>g</sub> β-Mn	-2.819	0.00	0.00	1.07	0.00	0.00	0.12	0.00	0.04	0.72	0.36	0.56	3.82	0.24

**Table 4** Molecular Orbital composition for Sn<sub>12</sub>Cu in the range of -(10.2-2.82) eV on the PBE0/cc-pVTZ-PP level of theory. The absolute coefficients are displayed, equivalent atomic orbitals (AO) and ligands have been summarized.

Label	E/eV	Cu-3s	Cu-3p	Cu-3d	Cu-4s	Cu-4p	Cu-4d	Sn-4s	Sn-4p	Sn-4d	Sn-4f	Sn-5s	Sn-5p	Sn-5d
1E <sub>u</sub> $\alpha$ -Cu	-10.019	0.00	0.00	0.00	0.00	0.00	0.00	0.00	0.00	0.66	0.00	2.10	0.50	0.32
1E <sub>u</sub> $\alpha$ -Cu	-10.019	0.00	0.00	0.00	0.00	0.00	0.00	0.00	0.00	0.64	0.02	2.02	0.44	0.28
2A <sub>u</sub> $\alpha$ -Cu	-9.831	0.00	0.01	0.00	0.00	0.02	0.00	0.00	0.00	0.56	0.02	2.40	0.74	0.34
3E <sub>g</sub> $\alpha$ -Cu	-9.173	0.00	0.00	1.73	0.00	0.00	0.00	0.00	0.00	0.18	0.00	0.58	0.84	0.04
3E <sub>g</sub> $\alpha$ -Cu	-9.173	0.00	0.00	1.91	0.00	0.00	0.00	0.00	0.00	0.24	0.02	0.56	0.78	0.04
4A <sub>u</sub> $\alpha$ -Cu	-9.159	0.00	0.00	2.25	0.03	0.00	0.02	0.00	0.00	0.16	0.04	0.46	1.00	0.02
5E <sub>g</sub> $\alpha$ -Cu	-9.110	0.00	0.00	2.09	0.00	0.00	0.00	0.00	0.00	0.20	0.00	0.52	0.70	0.00
5E <sub>g</sub> $\alpha$ -Cu	-9.110	0.00	0.00	1.52	0.00	0.00	0.00	0.00	0.00	0.18	0.00	0.52	0.82	0.02
6A <sub>g</sub> $\alpha$ -Cu	-8.460	0.15	0.00	0.20	0.31	0.00	0.12	0.00	0.04	0.90	0.46	0.96	3.56	0.18
7E <sub>u</sub> $\alpha$ -Cu	-7.197	0.00	0.01	0.00	0.00	0.00	0.00	0.00	0.00	0.82	0.38	0.08	4.72	0.06
7E <sub>u</sub> $\alpha$ -Cu	-7.195	0.00	0.01	0.00	0.00	0.00	0.00	0.00	0.00	0.82	0.30	0.06	4.82	0.06
8E <sub>u</sub> $\alpha$ -Cu	-7.089	0.00	0.00	0.00	0.00	0.00	0.00	0.00	0.00	0.74	0.24	0.00	4.94	0.08
8E <sub>u</sub> $\alpha$ -Cu	-7.089	0.00	0.00	0.00	0.00	0.00	0.00	0.00	0.00	0.86	0.30	0.00	5.00	0.08
9A <sub>u</sub> $\alpha$ -Cu	-6.338	0.00	0.40	0.00	0.00	0.08	0.00	0.00	0.00	0.72	0.34	0.60	4.30	0.12
10E <sub>u</sub> $\alpha$ -Cu	-6.261	0.00	0.31	0.00	0.00	0.04	0.00	0.00	0.00	0.68	0.32	0.64	4.16	0.18
10E <sub>u</sub> $\alpha$ -Cu	-6.261	0.00	0.33	0.00	0.00	0.05	0.00	0.00	0.00	0.80	0.32	0.66	4.14	0.08
11E <sub>g</sub> $\alpha$ -Cu	-5.608	0.00	0.00	0.33	0.00	0.00	0.01	0.00	0.00	0.44	0.34	0.96	4.90	0.10
11E <sub>g</sub> $\alpha$ -Cu	-5.608	0.00	0.00	0.36	0.00	0.00	0.03	0.00	0.00	0.54	0.40	0.96	5.16	0.12
12E <sub>g</sub> $\alpha$ -Cu	-5.543	0.00	0.00	0.37	0.00	0.00	0.01	0.00	0.00	0.44	0.32	0.96	5.02	0.12
12E <sub>g</sub> $\alpha$ -Cu	-5.543	0.00	0.00	0.37	0.00	0.00	0.01	0.00	0.00	0.44	0.42	0.92	4.90	0.08
13A <sub>g</sub> $\alpha$ -Cu	-5.404	0.02	0.00	0.34	0.01	0.00	0.02	0.00	0.00	0.52	0.28	0.80	5.12	0.06
1E <sub>u</sub> $\beta$ -Cu	-9.948	0.00	0.00	0.00	0.00	0.00	0.00	0.00	0.02	0.60	0.02	2.10	0.48	0.28
1E <sub>u</sub> $\beta$ -Cu	-9.948	0.00	0.00	0.00	0.00	0.00	0.00	0.00	0.00	0.56	0.02	2.06	0.40	0.28
2A <sub>u</sub> $\beta$ -Cu	-9.587	0.00	0.00	0.00	0.00	0.02	0.00	0.00	0.00	0.56	0.02	2.38	0.70	0.36
3E <sub>g</sub> $\beta$ -Cu	-9.159	0.00	0.00	1.77	0.00	0.00	0.00	0.00	0.00	0.18	0.00	0.56	0.84	0.04
3E <sub>g</sub> $\beta$ -Cu	-9.159	0.00	0.00	2.09	0.00	0.00	0.00	0.00	0.00	0.22	0.00	0.58	0.82	0.06
4E <sub>g</sub> $\beta$ -Cu	-9.091	0.00	0.00	1.79	0.00	0.00	0.00	0.00	0.00	0.22	0.00	0.54	0.76	0.02
4E <sub>g</sub> $\beta$ -Cu	-9.091	0.00	0.00	2.16	0.00	0.00	0.00	0.00	0.00	0.16	0.00	0.56	0.78	0.02
5A <sub>g</sub> $\beta$ -Cu	-8.982	0.01	0.00	2.24	0.01	0.00	0.06	0.00	0.00	0.22	0.04	0.56	1.06	0.02
6A <sub>g</sub> $\beta$ -Cu	-8.387	0.14	0.00	0.15	0.31	0.00	0.12	0.00	0.04	0.94	0.40	0.98	3.54	0.20
7G <sub>u</sub> $\beta$ -Cu	-7.037	0.00	0.05	0.00	0.00	0.00	0.00	0.00	0.00	0.82	0.38	0.16	5.14	0.08
7G <sub>u</sub> $\beta$ -Cu	-7.037	0.00	0.05	0.00	0.00	0.00	0.00	0.00	0.00	0.76	0.32	0.12	5.18	0.06
7G <sub>u</sub> $\beta$ -Cu	-7.026	0.00	0.00	0.00	0.00	0.00	0.00	0.00	0.00	0.80	0.30	0.00	4.68	0.12
7G <sub>u</sub> $\beta$ -Cu	-7.026	0.00	0.00	0.00	0.00	0.00	0.00	0.00	0.00	0.78	0.32	0.00	4.78	0.08
8E <sub>u</sub> $\beta$ -Cu	-6.210	0.00	0.36	0.00	0.00	0.07	0.00	0.00	0.00	0.74	0.36	0.64	4.12	0.15
8E <sub>u</sub> $\beta$ -Cu	-6.210	0.00	0.44	0.00	0.00	0.08	0.00	0.00	0.00	0.74	0.38	0.64	4.24	0.08
9A <sub>u</sub> $\beta$ -Cu	-6.076	0.00	0.43	0.00	0.00	0.09	0.00	0.00	0.00	0.78	0.30	0.56	4.34	0.14
10E <sub>g</sub> $\beta$ -Cu	-5.578	0.00	0.00	0.32	0.00	0.00	0.01	0.00	0.00	0.42	0.32	0.96	4.96	0.10
10E <sub>g</sub> $\beta$ -Cu	-5.578	0.00	0.00	0.38	0.00	0.00	0.02	0.00	0.00	0.50	0.42	0.98	5.24	0.12
11E <sub>g</sub> $\beta$ -Cu	-5.475	0.00	0.00	0.34	0.00	0.00	0.02	0.00	0.00	0.40	0.44	0.92	4.86	0.14
11E <sub>g</sub> $\beta$ -Cu	-5.472	0.00	0.00	0.24	0.00	0.00	0.01	0.00	0.00	0.36	0.36	0.96	5.08	0.12
12A <sub>g</sub> $\beta$ -Cu	-4.174	0.01	0.00	0.31	0.04	0.00	0.01	0.02	0.00	0.48	0.32	0.84	5.12	0.12

**Table 5** Molecular Orbital composition for Sn<sub>12</sub>Au in the range of -(10.2-2.82) eV on the PBE0/cc-pVTZ-PP level of theory. The absolute coefficients are displayed, equivalent atomic orbitals (AO) and ligands have been summarized.

Label	E/eV	Au-4f	Au-5s	Au-5p	Au-5d	Au-5f	Au-6s	Au-6p	Au-6d	Sn-4s	Sn-4p	Sn-4d	Sn-4f	Sn-5s	Sn-5p	Sn-5d
1E <sub>u</sub> α-Au	-10.063	0.00	0.00	0.00	0.00	0.02	0.00	0.00	0.00	0.00	0.52	0.04	2.10	0.40	0.24	
1E <sub>u</sub> α-Au	-10.063	0.00	0.00	0.00	0.00	0.02	0.00	0.00	0.00	0.02	0.50	0.04	2.00	0.36	0.26	
2A <sub>u</sub> α-Au	-9.981	0.00	0.00	0.00	1.88	0.00	0.00	0.00	0.10	0.00	0.34	0.02	1.10	1.20	0.20	
3E <sub>u</sub> α-Au	-9.981	0.00	0.00	0.00	1.91	0.00	0.00	0.00	0.10	0.00	0.32	0.04	1.12	1.20	0.18	
3E <sub>g</sub> α-Au	-9.946	0.00	0.00	0.00	1.58	0.00	0.00	0.00	0.08	0.00	0.26	0.00	1.10	1.26	0.16	
4A <sub>u</sub> α-Au	-9.946	0.00	0.00	0.00	1.84	0.00	0.00	0.00	0.09	0.00	0.30	0.06	1.10	1.14	0.14	
5E <sub>g</sub> α-Au	-9.932	0.00	0.00	0.00	1.85	0.00	0.00	0.00	0.11	0.00	0.38	0.06	1.00	1.50	0.08	
5E <sub>g</sub> α-Au	-9.927	0.00	0.00	0.00	0.00	0.01	0.00	0.01	0.00	0.00	0.60	0.02	2.40	0.60	0.32	
6A <sub>g</sub> α-Au	-9.083	0.00	0.11	0.00	0.43	0.00	0.29	0.00	0.24	0.00	0.02	0.96	0.34	1.10	2.98	0.16
7E <sub>u</sub> α-Au	-7.091	0.00	0.00	0.00	0.00	0.02	0.00	0.10	0.00	0.00	0.88	0.32	0.04	4.76	0.04	
7E <sub>u</sub> α-Au	-7.091	0.00	0.00	0.00	0.00	0.02	0.00	0.11	0.00	0.00	0.80	0.34	0.06	4.98	0.04	
8E <sub>u</sub> α-Au	-6.991	0.00	0.00	0.00	0.00	0.03	0.00	0.00	0.00	0.00	0.82	0.26	0.00	4.92	0.02	
8E <sub>u</sub> α-Au	-6.991	0.00	0.00	0.00	0.00	0.02	0.00	0.00	0.00	0.00	0.82	0.34	0.00	4.84	0.06	
9A <sub>u</sub> α-Au	-6.316	0.05	0.00	0.10	0.00	0.18	0.00	1.57	0.00	0.00	0.06	0.66	0.46	0.72	4.38	0.16
10E <sub>u</sub> α-Au	-6.245	0.04	0.00	0.08	0.00	0.17	0.00	1.44	0.00	0.00	0.04	0.70	0.44	0.64	3.74	0.10
10E <sub>u</sub> α-Au	-6.245	0.05	0.00	0.09	0.00	0.17	0.00	1.53	0.00	0.00	0.00	0.62	0.42	0.64	3.96	0.16
11E <sub>g</sub> α-Au	-5.453	0.00	0.00	0.00	0.50	0.00	0.00	0.00	0.07	0.00	0.00	0.46	0.40	0.92	5.64	0.10
11E <sub>g</sub> α-Au	-5.453	0.00	0.00	0.00	0.47	0.00	0.00	0.00	0.06	0.00	0.00	0.48	0.44	0.90	4.90	0.14
12E <sub>g</sub> α-Au	-5.423	0.00	0.00	0.00	0.39	0.00	0.00	0.00	0.06	0.00	0.00	0.38	0.36	0.92	4.90	0.08
12E <sub>g</sub> α-Au	-5.423	0.00	0.00	0.00	0.46	0.00	0.00	0.00	0.06	0.00	0.00	0.42	0.38	0.90	5.06	0.12
13A <sub>g</sub> α-Au	-5.358	0.00	0.00	0.00	0.42	0.00	0.02	0.00	0.07	0.02	0.00	0.53	0.32	0.80	5.66	0.08
1E <sub>u</sub> β-Au	-9.987	0.00	0.00	0.00	0.00	0.02	0.00	0.00	0.00	0.00	0.52	0.04	2.11	0.38	0.24	
1E <sub>u</sub> β-Au	-9.987	0.00	0.00	0.00	0.00	0.02	0.00	0.00	0.00	0.02	0.50	0.04	2.01	0.38	0.26	
2E <sub>g</sub> β-Au	-9.946	0.00	0.00	0.00	1.88	0.00	0.00	0.00	0.10	0.00	0.00	0.32	0.02	1.13	1.22	0.20
2E <sub>g</sub> β-Au	-9.946	0.00	0.00	0.00	1.86	0.00	0.00	0.00	0.10	0.00	0.00	0.32	0.04	1.16	1.26	0.22
3E <sub>g</sub> β-Au	-9.910	0.00	0.00	0.00	1.57	0.00	0.00	0.00	0.08	0.00	0.00	0.26	0.00	1.10	1.28	0.16
3E <sub>g</sub> β-Au	-9.910	0.00	0.00	0.00	1.83	0.00	0.00	0.00	0.09	0.00	0.00	0.28	0.06	1.10	1.22	0.14
4A <sub>g</sub> β-Au	-9.763	0.00	0.01	0.00	1.84	0.00	0.02	0.00	0.11	0.00	0.00	0.40	0.08	1.10	1.52	0.10
5A <sub>u</sub> β-Au	-9.717	0.00	0.00	0.00	0.00	0.01	0.00	0.04	0.00	0.00	0.00	0.62	0.02	2.40	0.68	0.34
6A <sub>g</sub> β-Au	-9.021	0.00	0.11	0.00	0.42	0.00	0.29	0.00	0.24	0.00	0.02	0.98	0.34	1.14	2.96	0.18
7G <sub>u</sub> β-Au	-6.925	0.00	0.00	0.00	0.00	0.03	0.00	0.00	0.00	0.00	0.00	0.82	0.24	0.00	4.92	0.02
7G <sub>u</sub> β-Au	-6.925	0.00	0.00	0.00	0.00	0.02	0.00	0.00	0.00	0.00	0.00	0.82	0.28	0.00	4.80	0.06
7G <sub>u</sub> β-Au	-6.917	0.00	0.00	0.01	0.00	0.03	0.00	0.18	0.00	0.00	0.00	0.88	0.36	0.12	4.82	0.04
7G <sub>u</sub> β-Au	-6.917	0.00	0.00	0.01	0.00	0.03	0.00	0.20	0.00	0.00	0.00	0.76	0.32	0.12	4.90	0.06
8E <sub>u</sub> β-Au	-6.199	0.04	0.00	0.08	0.00	0.16	0.00	1.41	0.00	0.00	0.04	0.64	0.38	0.62	3.66	0.10
8E <sub>u</sub> β-Au	-6.196	0.05	0.00	0.09	0.00	0.17	0.00	1.47	0.00	0.00	0.00	0.74	0.42	0.64	4.06	0.14
9A <sub>u</sub> β-Au	-6.109	0.05	0.00	0.10	0.00	0.18	0.00	1.59	0.00	0.00	0.02	0.70	0.48	0.66	4.46	0.20
10E <sub>g</sub> β-Au	-5.421	0.00	0.00	0.00	0.50	0.00	0.00	0.07	0.00	0.00	0.46	0.38	0.92	5.68	0.10	
10E <sub>g</sub> β-Au	-5.421	0.00	0.00	0.00	0.47	0.00	0.00	0.06	0.00	0.00	0.46	0.44	0.90	4.88	0.12	
11E <sub>g</sub> β-Au	-5.350	0.00	0.00	0.00	0.41	0.00	0.00	0.00	0.06	0.00	0.40	0.42	0.92	4.90	0.10	
11E <sub>g</sub> β-Au	-5.350	0.00	0.00	0.00	0.44	0.00	0.00	0.00	0.07	0.00	0.42	0.38	0.88	5.00	0.14	
12A <sub>g</sub> β-Au	-4.174	0.00	0.01	0.00	0.40	0.00	0.01	0.00	0.04	0.02	0.00	0.52	0.36	0.82	5.62	0.08